Lipidomics profiling of zebrafish liver through untargeted liquid chromatography-high resolution mass spectrometry

Iturrospe, Elias; Da Silva, Katyeny Manuela; van den Boom, Rik; van de Lavoir, Maria; Robeyns, Rani; Vergauwen, Lucia; Knapen, Dries; Cuykx, Matthias; Covaci, Adrian ; L.N. van Nuijs, Alexander

Published in:
Journal of Separation Science

DOI:
10.1002/jssc.202200214

Publication date:
2022

License:
Unspecified

Document Version:
Accepted author manuscript

Lipidomics profiling of zebrafish liver through untargeted liquid chromatography-high resolution mass spectrometry

Katyeny Manuela da Silva [1]*, Elias Iturrospe [1,2], Rik van den Boom [3], Maria van de Lavoir [1], Rani Robeyns [1], Lucia Vergauwen [3], Dries Knapen [3], Matthias Cuykx [1,4], Adrian Covaci [1], Alexander L.N. van Nuijs [1]*

[1] Toxicological Centre, Department of Pharmaceutical Sciences, University of Antwerp, Universiteitsplein 1, 2610 Antwerp, Belgium
[2] Department of In Vitro Toxicology and Dermato-Cosmetology, Faculty of Medicine and Pharmacy, Campus Jette, Vrije Universiteit Brussels, Laarbeeklaan 103, 1090 Brussels, Belgium
[3] Zebrafishlab, Veterinary Physiology and Biochemistry, Department of Veterinary Sciences, University of Antwerp, Universiteitsplein 1, 2610 Antwerp, Belgium
[4] Department of Laboratory Medicine AZ Turnhout. Rubenslaan 166, 2300 Turnhout, Belgium

*** - Corresponding authors**
Alexander L.N. van Nuijs. E-mail: alexander.vannuijs@uantwerpen.be
Katyeny Manuela Da Silva. E-mail: katyenymanuela.dasilva@uantwerpen.be

Running title: Strategies to evaluate LC-MS based lipidomics methods in zebrafish

Keywords: Model organism; Danio rerio; Lipid extraction; Sample preparation; Tandem mass spectrometry.

Abbreviations: CAR: Carnitine. Cer: Ceramide. DG: Diacylglycerol. dQC: Pooled sample dilution. FA: Fatty acid. HE: In House Extraction, MeOH/$CHCl_3$/H_2O (3/2/2, v/v/v). LPA: Lysophosphatidic acid. LPC: Lysophosphatidylcholine. LPE: Lysophosphatidylethanolamine. LPI: Lysophosphatidylinositol. *M*: Average. ME: Matyash Extraction, MeOH/MTBE/H_2O (3/10/2.5, v/v/v). MHE: Modified House Extraction, MeOH/CH_2Cl_2/H_2O (2/3/2, v/v/v). NAE: N-acylethanolamine. PA: Glycerophosphatidic acid. PC: Glycerophosphocholine. PE: Glycerophosphoethanolamine. PG: Glycerophosphoglycerol. PI: Glycerophosphoinositol. PS: Glycerophosphoserine. *SD*: Standard deviation. SM: Sphingomyelin. TG: Triacylglycerol.

Abstract

Lipidomics analysis of zebrafish tissues has shown promising results to understand disease-related outcomes of exposure to toxic substances at molecular level. However, knowledge about their lipidome is limited, as most untargeted studies only identify the lipids that are statistically significant in their setup. In this work, liquid chromatography-high resolution mass spectrometry was used to study different aspects of the analytical workflow, i.e., extraction solvents (methanol/chloroform/water (3/2/2, v/v/v), methanol/dichloromethane/water (2/3/2, v/v/v) and methanol/methyl-tert-butyl ether/water (3/10/2.5, v/v/v), instrumental response, and strategies used for lipid annotation. The number of high-quality features (relative standard deviation of the intensity values ≤ 10% in the range 10^3–10^7 counts) was affected by the dilution of lipid extracts, indicating that it is an important parameter for developing untargeted methods. The workflows used allowed the selection of a dilution factor to annotate 712 lipid species (507 bulk lipids) in zebrafish liver using four software (LipidMatch, LipidHunter, MS-DIAL and Lipostar). Retention time mapping was a valuable tool to filter lipid annotations obtained from automatic software annotations. The lipid profiling of zebrafish livers will help in a better understanding of the true constitution of their lipidome at the species level, as well as in the use of zebrafish in toxicological studies.

1. Introduction

Zebrafish (*Danio rerio*) is a low-cost, medium-to-high throughput model organism used in toxicological and ecotoxicological research to investigate the acute and long-term effects of exposure to chemicals. Apart from the lack of a stomach, the zebrafish digestive system is highly similar to that of mammals including humans, both structurally and functionally. Metabolic functions and processes are also highly conserved, including the major metabolic pathways and hormones regulating e.g., digestion, appetite, and glucose homeostasis (Benchoula et al., 2019; da Silva, Iturrospe, Bars, et al., 2021). Zebrafish are increasingly being used to study the effects of so-called metabolic disruptors, a class of endocrine-disrupting compounds that increase the susceptibility to metabolic disorders. Amongst others, exposure to metabolic disruptors can result in dysregulation of lipid metabolism, including aberrant lipid accumulation and altered lipid and fatty acid profiles in tissues, such as the liver (Sun et al., 2020). In recent years, the number of studies combining the zebrafish model with omics techniques has grown considerably, showing the potential of these techniques to provide relevant and complementary information for safety assessments (Lai et al., 2021).

Lipidomics, a sub-discipline of metabolomics that investigates the composition of lipids and their biological relevance in a biological system, has shown important developments for *in vitro* and *in vivo* exposure studies and many other applications (Cajka & Fiehn, 2014). With advancements in analytical techniques to characterize lipid species, the development of a classification system (LIPID MAPS classification hierarchy), and bioinformatics tools focused on lipid pathways, the lipidomics field has rapidly advanced (Liebisch et al., 2013). The most commonly used lipidomics strategy consists of extraction using organic solvents, followed by reversed-phase liquid chromatography-mass spectrometry (RPLC-MS) (Cajka & Fiehn, 2014; Witting & Böcker, 2020). Untargeted high resolution mass spectrometry (HRMS) methods combined with liquid-liquid extraction (LLE) provide comprehensive coverage of multiple lipid classes (da Silva, Iturrospe, Bars, et al., 2021; Hyötyläinen, 2021). In many applications, sample preparation methods developed for a specific sample type will be applied to a different matrix. Changing the sample type can influence the method's efficiency and coverage (Ulmer et al., 2018), but the evaluation of this effect using untargeted methods is extremely challenging since various compounds are affected differently (Liu et al., 2021; Sands et al., 2021).

The use of automated lipid annotation can help to evaluate which classes were extracted and the number of different species, helping to rapidly assess the effect of different experimental conditions. Currently, the gold standard used for automated lipid species annotation is based

on rule-based fragmentation when collision-induced dissociation is used (Koelmel, Kroeger, Ulmer, et al., 2017; Köfeler et al., 2021). However, lipid annotation in biological samples with high lipid content (e.g., liver, plasma) is extremely challenging due to the number of isobaric and isomeric species with similar fragments and in-source fragmentation which can generate lipid species from a different subclass (Criscuolo et al., 2020).

Model organisms play a significant role in understanding the functions of lipids. Qualitative information on lipid composition that can be used for further quantitative measurements to study metabolic diseases and exposure to toxicants is of special interest since this information is still scarce (da Silva, Iturrospe, Bars, et al., 2021). In this study, an analytical workflow for zebrafish liver tissues was explored using an untargeted RPLC-HRMS-based platform previously applied for liver cell extracts (da Silva, Iturrospe, Heyrman, et al., 2021). Different mixtures of organic solvents were tested for lipid extraction: in house extraction (HE) method (modified Bligh-Dyer (Bligh & Dyer, 1959)) consisting of methanol (MeOH)/chloroform ($CHCl_3$)/water (H_2O) (3/2/2, v/v/v) and previously optimized for the HepaRG liver cell line (Cuykx, Mortelé, et al., 2017; Iturrospe et al., 2022), a modified in house extraction (MHE) method consisting of MeOH/dichloromethane (CH_2Cl_2)/H_2O (2/3/2, v/v/v) and the Matyash *et al* (Matyash et al., 2008) extraction (ME) using MeOH/methyl-tert-butyl ether (MTBE)/H_2O (3/10/2.5, v/v/v). The MHE and ME methods were tested to evaluate the replacement of chloroform for a less harmful solvent, as previously reported for a lipidomics application using zebrafish muscle (Arribat et al., 2020). Additionally, the effect of the dilution of the extracts on the response of different lipid classes, mass accuracy, and the number of high-quality features were evaluated. The annotation of lipid species using *in silico* libraries was evaluated using well-recognized software tools for lipidomics, i.e., MS-DIAL ver. 4.70 (Tsugawa et al., 2020), LipidMatch 3.0 (Koelmel, Kroeger, Ulmer, et al., 2017), LipidHunter 2 (Ni, Angelidou, Lange, et al., 2017) and Lipostar 2.0 (Goracci et al., 2017).

2. Materials and methods

2.1 Chemicals

The solvents MeOH, acetonitrile (MeCN), and formic acid (HCOOH, 99%) UPLC-MS grade were purchased from Biosolve (Valkenswaard, The Netherlands). Ammonium formate (NH_4COOH) and ammonium acetate (NH_4COOCH_3), both LC-MS grade, were obtained from Sigma Aldrich (St. Louis, USA). Acetic acid ($HCOOCH_3$, LC-MS grade), isopropanol (IPA, ACS reagent), ammonia solution (NH_4OH 25%, LC-MS grade), $CHCl_3$ (analytical grade), CH_2Cl_2 (analytical grade), and MTBE (analytical grade) were purchased from Merck (Merck

KGaA, Darmstadt, Germany). Ultrapure water (H_2O, 18.2 MΩ) was obtained from an Elga Pure Lab apparatus (Tienen, Belgium). Tricaine methanesulfonate (MS-222) was obtained from Sigma Aldrich. Internal standards (IS) were used in different steps of the sample preparation and are described as internal standards-I (IS-I) and internal standards-II (IS-II). IS-I refers to the following labeled standards: glyceryl tri(palmitate-1-^{13}C) (TG 16:0/16:0/16:0-$^{13}C_3$) and cholic acid-2,2,4,4-D_4 (ST 24:1;O5-D_4) both purchased from Sigma Aldrich, lauric acid-12,12,12-D_3 (FA 12:0-D_3) from CDN Isotopes (Pointe-Claire, Quebec, Canada), 1-oleoyl(D7)-2-hydroxy-sn-glycero-3-phosphoethanolamine (LPE 18:1-D7) from Avanti Polar Lipids (Alabaster, USA) and octanoyl-L-carnitine-(N-methyl-D_3) (CAR 8:0-D_3) and N-oleoyl($^{13}C_{18}$)-D-sphingosine (Cer d18:1/18:1(9Z)-$^{13}C_{18}$) from Cambridge Isotope Laboratories (Massachusetts, USA). IS-II refers to SPLASH Lipidomix from Avanti Polar Lipids (Table SI-1.1).

2.2 Sample collection

Six-month old zebrafish (*Danio rerio*, AB strain) were reared in an automatic housing system (ZebTec standalone, Tecniplast, Buguggiate, Italy) with a 14:10 h light: dark cycle and recirculating, biologically filtered water (28 ± 0.2 °C, pH 7.5 ± 0.3 and conductivity 500 ± 15 µS/cm), as previously described (Michiels et al., 2019). Reconstituted freshwater (45 mg/L $CaCO_3$) was prepared by adding Instant Ocean Sea Salt (Instant Ocean) to reverse-osmosis water (RO 40; Werner). Ammonium, nitrite, and nitrate levels were measured twice a week and remained below 0.25, 0.3, and 12.5 mg/L, respectively. Fish were fed twice a day with dry feed (Zebrafeed, Sparos, Portugal) and once a day with frozen feed (*Artemia* sp., *Daphnia* sp., *Chironomidae*, and *Chaoboridae* larvae; Aquaria Antwerp, Antwerpen, Belgium). Fish were euthanized by immersion in a solution of MS-222 (300 mg/L, pH 7.5) until loss of opercular movement, followed by decapitation. The fish were collected from the tank, euthanized, and dissected one after the other to limit the postmortem formation/degradation of metabolites. The liver was collected in pre-weighed cryo-vial tubes (Cryo.S, Greiner Bio-One, Kremsmünster, Austria), weighed, and immediately quenched in liquid nitrogen. The frozen tissues were stored at −80 °C until the remaining fish were dissected before proceeding with the sample preparation. The experiments described in this work (two batches using six analytical replicates for each extraction method) required the use of 27 zebrafishes (440.9 mg of wet tissue). Fish husbandry and experiments were carried out in strict accordance with EU Directive 2010/63/

EU on the protection of animals used for scientific purposes ("Directive 2010/63/EU on the Protection of Animals Used for Scientific Purposes," 2010).

2.3 Sample preparation

Samples were kept on dry ice after removal from the −80 °C freezer for sample preparation. Frozen liver samples were homogenized with a mixture of MeOH/H_2O (1/2, v/v, 20 µL/mg of wet tissue) containing the IS-I mixture (7 µg/mL) in 2.0 mL BeadBug tubes prefilled with 0.1 mm silica glass beads (Merck KGaA, Darmstadt, Germany). A Precellys-24 tissue homogenizer (Bertin Technologies, Montigny-le-Bretonneux, France) was used to homogenize the samples at 5,000 Hz for two cycles of 20 s with a 10 s break between cycles. The homogenate of different individuals was mixed to obtain a pooled sample (Figure SI-1). The pooled samples were first divided into 10 mg-equivalents of tissue by transferring 200 µL to different LLE glass with the correspondent organic solvent mixture (MeOH/$CHCl_3$ (57/43, v/v) for HE, MeOH/$CHCl_2$ (36/64, v/v) for MHE, or MeOH/MTBE (19/81, v/v) for ME) previously stored at -20 °C. The samples were vortexed for 20 s and H_2O was added to each sample to obtain the final solvent ratios MeOH/$CHCl_3$/H_2O (3/2/2, v/v/v) for HE, MeOH/CH_2Cl_2/H_2O (2/3/2, v/v/v) for MHE and MeOH/MTBE/H_2O (3/10/2.5, v/v/v) for ME. Next, they were vortexed for 20 s, equilibrated for 10 min at 4 °C, and centrifuged at 2200 g for 5 min. After centrifugation, 400 µL of the upper-phase of the ME LLE vials and 300 µL of the lower-phase of the MHE and HE LLE vials were collected and dried under N_2. The extracts were resuspended in a mixture of IPA/MeOH (150 µL, 35/65, v/v) with the IS-II, vortexed for 30 s, and filtered with 0.2 µm centrifugal filters (centrifuged at 7,000 g for 2 min). Six analytical replicates were used for each extraction method. For the dilution series experiment, pooled mixtures (referred to as quality control samples (QC)) of each extraction (HE, MHE, ME) were prepared by collecting an aliquot of each replicate of filtered extracts (30 µL). The QC mixtures were further diluted with the reconstitution solvent (IPA/MeOH, 35/65, v/v) to the respective factors: no dilution (dQC_1), 1/2 (dQC_2), 1/4 (dQC_3), 1/8 (dQC_4), and 1/16 (dQC_5).

2.4 Instrumental analysis

Analytical measurements were performed on an Agilent 1290 Infinity II LC system coupled to an Agilent 6560 drift tube-ion mobility-quadrupole-time-of-flight high resolution mass spectrometer (DTIM-QToF-HRMS) (Agilent Technologies, Santa Clara, USA) using Agilent Dual Jet Stream Electrospray Ionization (ESI) in positive (+) and negative modes (−), as

previously described (da Silva, Iturrospe, Heyrman, et al., 2021). Data were acquired in 2 GHz extended dynamic mode with a scan range of 100-1700 *m/z* in profile mode. Ionization parameters were as follows: In ESI (+) mode, drying gas and sheath gas temperature 325 °C with a flow rate of 8 L/min, nebulizer gas pressure 30 psig, Vcap 3500 V, nozzle voltage 500 V and fragmentor 200 V; in ESI (-) mode, the drying and sheath gas both had a temperature of 350 °C and flow rate of 8 L/min. The nebulizer gas pressure was 30 psig. The following voltages were applied: Vcap 3750 V, nozzle voltage 500 V, and fragmentor 200 V. Detailed parameters used for the analytical method are described in Table SI-1.2.

2.5 Data analysis

The LC-HRMS raw data files (Agilent .d format) were processed in MS-DIAL ver. 4.70 (Tsugawa et al., 2020). The resulting data matrix was uploaded to the MS-FLO web tool to remove duplicates and isotopic features (DeFelice et al., 2017). Drift correction, blank subtraction with the flag contaminants function (median of blanks > 0.2 * median of biological samples' intensities), and missing value imputation with random forest were performed using notame package in R (Klåvus et al., 2020). The relative standard deviation (RSD) values were calculated using the non-parametric formula (1.48 * (median absolute deviation ÷ median)) to evaluate the precision of the datasets generated by the different extraction methods (Broadhurst et al., 2018).

For lipid annotation, the *in silico* LipidBlast library (Tsugawa et al., 2020) was used in MS-DIAL ver. 4.70 for MS/MS spectra matching in addition to rule-based fragmentation tools, LipidMatch 3.0 (Koelmel, Kroeger, Ulmer, et al., 2017), LipidHunter 2 (Ni, Angelidou, Lange, et al., 2017) and Lipostar 2.0 (using the LIPID MAPS structure database of January 2022) (Goracci et al., 2017). For LipidMatch, the MS-DIAL/MS-FLO output was used with the raw MS/MS data to annotate lipids using an R-based workflow. Lipostar annotations were performed in the raw data directly imported and aligned using the default Agilent data-dependent acquisition (DDA) parameters in positive and negative modes. Blank filtering and automatic approval were used to keep structures of quality of 3-4 stars (lipid rule-based confidence system 1–4 (Goracci et al., 2017)). The detailed parameter settings for MS-DIAL/MS-FLO and additional information for LipidHunter and Lipostar can be found in Table SI-1.3. To refine annotation results, Kendrick mass defect to the hydrogen base (KMD[H]) against retention time plots was generated in R (Lange et al., 2021) and adapted to include a confidence interval region (linear smooth, level = 0.9) using the ggplot package (Wickham,

2016). Shorthand notation was used to report confidence in annotation as suggested by Liebisch *et al* (Liebisch et al., 2020) for mass spectrometry-derived lipid structures. After merging the datasets from different software, one ion species was kept for coverage comparisons, and the other detected species were reported in an additional column. Data visualization was performed in R 4.0.5 and Microsoft Excel 2108.

3. Results and Discussion

3.1 Extractions

The creation of a homogenous pooled sample was crucial to eliminate the biological variability allowing the assessment of only analytical variability (i.e., sample preparation and instrumental analysis). Different MeOH/H_2O ratios were initially tested to avoid protein precipitation or phase separation before the pooled sample could be distributed to different extraction methods. The ratio MeOH/H_2O (1/2, v/v) allowed proper homogenization and did not show precipitation (Figure SI-1.1). Vortexing and sonication of the liver tissues were initially tested, but due to the poor homogenization and sample aggregation in the tube surface and cap, further experiments were not conducted. Bead-based tissue homogenization was used since it has been found to be the most effective strategy for sample dispersion and lipid recovery (Höring et al., 2021).

For LLE, biphasic extraction methods were used since they showed better performance in terms of coverage and yield for different lipid categories (e.g., glycerolipids and sphingolipids) using zebrafish liver (Gegner et al., 2022) and better sample cleanup. Biphasic LLE has been applied in different studies aiming to generate a metabolome/lipidome atlas of tissues (Ding et al., 2021; Lange et al., 2021). Moreover, LLE also offers the advantage to use the polar fraction for metabolomics analyses with complementary separation techniques (i.e., hydrophilic interaction chromatography (Iturrospe et al., 2021)) with less interference from abundant lipids (Cuykx, Negreira, et al., 2017). The average weight of the 72 wet fish livers was 16.9 mg (*SD* = 8.7 mg). Therefore, 10 mg was selected as the starting point.

3.2 Dilution series of zebrafish pooled liver extracts

In the dilution experiment, the goal was to evaluate the response of the MS system to different dilution factors of three types of extraction solvents with variable solubilities. Depending on lipids of interest for a specific biological question, different lipid classes can be enriched or diluted. Therefore, the selection of the dilution levels that allow the detection of compounds within the (linear) dynamic range of the instrument is preferred (Wu et al., 2019).

After data pre-processing including blank filtration, the number of features was 11,441 (HE), 9,004 (ME), and 9,633 (MHE) for ESI (+) and 3,438 (HE), 3,009 (MHE) and 2,975 (ME) for ESI (–). Blank subtraction caused an average feature reduction of 52%, highlighting the importance of removing background signals with respective extraction blanks prepared in the same experimental conditions. To evaluate the correlation of the filtered features versus the dilution factors, the intensity values were log normalized, and features with Pearson correlation coefficients (for all consecutive dilution factors) higher than 0.9 were plotted (Figure 1). Low signal correlation can be associated with high intensities (saturation level), low precision at either low or high levels, or matrix effects. Comparing the percentage of features showing a high Pearson correlation ($|r| > 0.9$) with the blank filtered features, they later represented 17% for HE, 23% for MHE and 12% for ME in ESI (+), and 17% for HE, 19% for MHE, 15% for ME in ESI (–) of the number of features. In Figure 1, the number of high-quality features, within the range 10^3–10^7 counts and RSD lower than 10% in the three replicates of each dQC, is also shown to evaluate whether additional dilution (e.g., 1/32) could be used to avoid saturation of high abundant lipids. However, the number of high-quality features decreased on average 59% (SD = 3) in ESI (+) and 76% (SD = 9) in ESI (–) mode, which suggests that an additional dilution of dQC5 impairs the detection of hundreds of features, potentially low abundant lipids.

In addition to the feature's response, lipids from different classes were annotated in the zebrafish liver samples to investigate the effect of the dilution on the mass accuracy and signal response. An overview of the annotated lipids (26 lipid species, 13 in ESI (+) and 13 in ESI (–)) can be found in Table SI-1.4. A bar chart with the average mass error versus the dilution levels can be found in Figure SI-1.2. Overall, the mass accuracy was consistent with an average mass error below 5.0 ppm for the same lipids in the different methods from the most concentrated samples (dQC1) until dQC4 (except for extraction HE at dQC5 (5.4 ± 3.1 ppm). The smooth regression lines in Figure SI-1.2. show a trend towards higher mass errors with a decrease in intensity for HE and MHE. For ME, this latter tendency can also be seen in the bar chart between dQC2-dQC5, while mass errors were higher at the dQC1 level (M = 4.5 ± 2.5 ppm) due to higher concentrations and possibly increased detector saturation.

Figure 2 shows the instrumental response of several classes of lipids, annotated at different dilution levels. While some lipid classes had a higher linear relationship (e.g., lysophosphatidylethanolamine (LPE)), others such as triacylglycerol (TG) in ESI (+) showed a non-linear behavior marked by saturation at lower dQC levels. In untargeted metabolomics

and lipidomics studies, intensities and/or peak areas are used to conduct statistical analysis to identify biologically relevant features for further structure elucidation. If these features are in the saturation or noise levels of the MS detector, statistical changes due to a biological condition may be overlooked.

Even with an optimal dilution factor, some species will still be in the saturation or noise levels, but this strategy allows to qualitatively assess mass accuracy, feature, and metabolite response and increase the global data quality in an untargeted setting. Furthermore, it is recommended to include dQC samples in untargeted experiments to assess discrepancies in compounds annotated with different ESI ion species (e.g., [M+Na]+, [M–H]–), as suggested by Sands *et al* (Sands et al., 2021). For lipids, some classes can be detected in both ESI (+) and (–) and as different ion species (e.g., sphingolipids and glycerophospholipids). When intensity differences are observed between sample groups in e.g. an exposure study for a specific adduct type of a lipid species, dQC could be used to investigate the discrepancy between the results for different adducts.

3.3 Lipidome coverage

Lipid annotations are essential to determine whether a sample preparation procedure is appropriate for an untargeted lipidomics study, or for adapting the method to alternative matrices. After data pre-processing (i.e., peak detection, feature alignment, blank filtration), the quality of the dataset was evaluated by the median relative standard deviation (mRSD) of the feature intensities using the dQC2 level. Six technical replicates acquired in full scan mode were used for each extraction method in ESI (+) and ESI (–) modes. The intensity values showed mRSD < 15% for on average 5,178 features in ESI (+) and 3,618 features in ESI (–) modes (Figure SI-1.3).

The annotation workflow for lipid species included matching of accurate mass and *in silico* MS/MS spectra, and retention time (RT) evaluation by plotting RT against the KMD[H] (Figure SI-1.4). The table with the 712 unique lipid species (507 bulk lipid species) from four LIPID MAPS categories (i.e., fatty acyls, glycerolipids, glycerophospholipids, and sphingolipids) annotated in zebrafish liver extracts can be found in SI-2. The high number of lipid species were obtained using the combination of 72 DDA injections in ESI (+) and 72 in ESI (–) (i.e., 20 iterative exclusion and 28 auto-MS/MS (with active exclusion window of 0.2 min after two spectra) for each extraction method). The iterative exclusion MS/MS (i.e., the precursor ions selected for MS/MS will be excluded during the subsequent acquisition) and

active exclusion mode (i.e., after the MS/MS spectra of a given precursor are acquired, the ion is ignored for a given time window within the same run) increase the lipidome coverage by increasing the number of precursor ions that undergo MS/MS and by reducing the number of redundant spectra (Koelmel, Kroeger, Gill, et al., 2017).

Triacylglycerols (27%) followed by PC (21%), glycerophosphoethanolamines (PE) (10%), diacylglycerols (DG) (9%), and lysoglycerophospholipids (7%) were the most frequently detected lipid classes in zebrafish liver. Although concentration values were not obtained to estimate the absolute composition, these results show an interesting translational aspect in terms of lipid diversity. For instance, in an untargeted study to characterize the lipid composition of human livers, Kotronen *et al* (Kotronen et al., 2010) found that TGs and glycerophospholipids (mainly PC and PE) were the main components, in addition to a higher diversity of minor lipid species such as lysoglycerophospholipids and sphingolipids which were also detected in zebrafish liver investigated in the current study. Figure 3 shows the annotated lipids in zebrafish liver homogenates using the different extraction methods in terms of (A) coverage (number of detected lipid species per class) and (B) total carbon chain and number of double bond equivalents.

Although untargeted methods aim to cover as many metabolites as possible, LC-HRMS methods are limited towards certain metabolite classes (e.g., lipid mediators such as oxylipins require specific sample treatment and high instrumental sensitivity (Reinicke et al., 2020)) (da Silva, Iturrospe, Bars, et al., 2021). Due to the structural diversity of lipids, different studies and analytical platforms should be combined to reveal the most accurate composition of a specific organism or tissue. Using a targeted approach, Gegner *et al* (Gegner et al., 2022) investigated different combinations of solvents to extracts polar metabolites and lipids in three model organisms (*Mus musculus, Drosophila melanogaster,* and *Danio rerio*). The authors detected 422 metabolites in zebrafish liver. Triacylglycerols and glycerophospholipids were also the most frequently detected lipids using the MTBE-based extraction, followed by other lipid classes such as carnitines (CAR), free fatty acids (FA), and sphingolipids.

A total of 583, 565, and 575 lipids were annotated using the HE, MHE, and ME methods, respectively. Figure SI-1.5 shows a pie chart with the distribution of lipid classes and Figure SI-6 the relationship between the different extraction methods as a Venn diagram. Of the total number of annotated lipids, 67% were present in all extraction methods. This later highlights that the three methods showed similar results in terms of the number of annotated lipids in addition to coverage of different lipid classes (Figure 3). Ten percent was only annotated in ME, 9% in HE, and 5% in MHE. From the lipid species exclusively present in ME, 61% belong

to the TG class, followed by 13% DG. For HE, these values were 37% for TG and 12% for both PE and PG. Meanwhile, MHE showed 35% TG and 25% PC. This shows that the MTBE-based extraction has a slightly higher tendency to extract a broader range of glycerolipids than the other extraction mixtures, probably due to a combination of polarity (logP of 0.9) and a substantially higher amount of organic solvent in the ME mixture. Unless the study is focused on TG, the most abundant lipid class in both human and zebrafish liver tissues (Gegner et al., 2022; Kotronen et al., 2010), choosing a method that favors its extraction may not be the best choice, as it may inhibit ionization of low abundant lipids competing during ESI (Lange et al., 2021; Narváez-Rivas & Zhang, 2016). For global lipidomics approaches, regardless the column length or type of interaction, lipids in complex extracts will always show co-elution and sample fractionation is currently the most successful strategy to minimize this effect (Lange et al., 2021; Lebold et al., 2014). By comparing the pairs, HE∩MHE showed the highest similarity in annotated lipid species (507 lipids) mainly due to lipid subclasses PC (37%) and TG (17%), followed by ME∩MHE (493 lipids) and HE∩ME (485 lipids). Notably, the logP of CH_2Cl_2 (1.4) is between the values of $CHCl_3$ (1.9) and MTBE (0.9) (Aldana et al., 2020), which could help to explain this intermedia similarity.

The potential to distinguish lipids not only by class but also by the carbon chain length and degree of unsaturation is one of the advantages of LC-MS-based lipidomics approaches (Liebisch et al., 2020). In Figure 3.B, the carbon chain length plotted against the double bond equivalents for the three extraction methods, shows a similar profile. This latter means that the three methods can extract structural similar distributed lipids within the same polarity range. One of the purposes of this work was to evaluate if the in house optimized extraction method (HE) based on $CHCl_3$ could be replaced by CH_2Cl_2 or MTBE-based extractions, MHE and ME, respectively. Based on the lipid composition percentages (Figure SI-1.5) and the number of annotated lipid species (Figure 3.A), the three methods showed similar profiles and as a result, the HE could be replaced by either ME or MHE. Furthermore, if the polar fraction is of interest for metabolomics analysis, MHE would be preferable, as the bottom fraction in ME is relatively limited and difficult to separate from the precipitated proteins in tissue extracts.

3.4 Comparison of software for lipid annotation in zebrafish liver tissues

Annotation is a critical step of untargeted applications and different levels of confidence have been proposed to report the results based on the structural level (Liebisch et al., 2013) and analytical technique used (Alseekh et al., 2021). Usage of (I) the shorthand notation classification system (Liebisch et al., 2020), (II) RT mapping, (III) rule-based MS/MS spectra

matching, and (IV) indicating the software used for annotation are considered the golden standards for reporting qualitative lipidomics data. Different open-source software can be used to annotate lipids in untargeted datasets based on accurate mass measurements and MS/MS spectra matching (e.g., LipidMatch (Koelmel, Kroeger, Ulmer, et al., 2017), LipidHunter (Ni, Angelidou, Lange, et al., 2017), MS-DIAL (Tsugawa et al., 2020)). Given the known behavior of lipids in reversed-phase chromatographic columns (Lange et al., 2019), RT mapping has proved to be a valuable tool to reduce the number of false positives generated by in-source fragmentation and to facilitate unequivocal lipid annotation (Köfeler et al., 2021). For example, Lipostar (Goracci et al., 2017) is a software that includes RT mapping of lipid species against the KMD(H), but open-source scripts (Lange et al., 2021) can also be used after lipid annotation provided by other software.

Since data transformation and understanding the functionalities and parameters of each software are time-consuming steps that can also increase the complexity of the data analysis, software that provides a broad lipid coverage with fewer false positives would be ideal from a method development standpoint. In this work, different software platforms were used for lipid annotation to evaluate their similarity and complementarity (SI-2). Next to the compared annotation software, there are many others (e.g., lipid search module for MZmine (Korf et al., 2019), LDA (Hartler et al., 2017)), and a wide range of settings that can be optimized to improve performance. However, the evaluation of this four software can be very important for analytical laboratories that need to select one tool for method development using different sample types with an untargeted approach. Three open-source software, MS-DIAL, LipidMatch, and LipidHunter, and one commercial, Lipostar, were used to annotate 193, 311, 206, and 433 features, respectively. These latter numbers were derived after filtering out possible false positives based on RT mapping. Figure 4 illustrates the number of lipid species annotated with the software tools and their similarities using a Venn diagram.

LipidMatch and Lipostar showed the highest number of annotated lipid species after filtering, and also the highest similarity (33%) when comparing the pairs, followed by MSDIAL∩LipidMatch (29%) and MSDIAL∩Lipostar (25%). Alternatively, LipidHunter was the most complementary since its intersection with the other software showed lower values, LipidHunterL∩LipidMatch (15%), LipidHunterL∩MSDIAL (16%), and LipidHunterL∩Lipostar (16%). In practice, LipidHunter does not provide a stand-alone solution, i.e., the individual files (MS/MS raw data) will be transformed to open-source format and the software will look for lipids from different classes in a single or batch mode. The resulting files will contain detailed information about the fragment ions used to confirm the

lipid structure which can be useful for confirming the structure of lipids previously selected by statistical methods in untargeted datasets. In LipidMatch, the user has the option to run the R script with the feature table obtained from a different software package or process the files with the extension LipidMatch flow which uses MZmine for peak picking and alignment of multiple files in the background. In this work, the files were processed in MS-DIAL and the aligned feature table was exported to be used in LipidMatch. This strategy was beneficial since the user will have additional rule-based fragmentation in the same feature table already processed with the software of choice.

Interestingly, the few carnitine (CAR) and fatty acid (FA) lipid species (Figure SI-1.7) were all annotated using MS-DIAL. These lipids are very limited in terms of diversity and concentration in zebrafish liver tissues (Gegner et al., 2022). MS-DIAL algorithms could detect these species, CAR by the characteristic MS/MS spectra showing neutral loss of trimethylamine (TMA) and *m/z* 85.029 [M-fatty acid chain-TMA]+ (Figure SI-1.8). FAs were mainly annotated by accurate mass, isotopic distribution, and RT mapping. Figure SI-9 shows the MS/MS matching profile of different free FA obtained from MS-DIAL. While species such as FA 16:1 did not show fragmentation and its match was solely based on the precursor ion, elongated saturated species, such as FA 20:0, showed a neutral loss of water [M-H-H_2O]- at 20 eV (Murphy, 2014). Moreover, a highly unsaturated FA species, FA 22:6, was found in zebrafish livers showing extensive fragmentation. However, the MS-DIAL library did not provide any product ions that could be matched with the raw spectra (Figure SI-9).

Lipostar has noteworthy features that include isotopic clustering, allowing the combination of ion species from different polarities and visualization of fragment ions from the *in silico* predictions used to match with the structure of the lipid species (Ni, Angelidou, Hoffmann, et al., 2017). The detection of potentially oxidized lipids in positive mode for a given annotated lipid species is one of the advantages, as seen for some compounds in Table SI-2. For instance, TG 58:10 $[M+NH_4]^+$ was also detected as a potentially oxidized species $[M+O+NH_4]^+$ (960.7656). Figure SI-1.10 shows the MS/MS spectra of the unmodified and oxidized TG 58:10 $[M+ NH_4]^+$. The compound was annotated based on the ammonia neutral loss, the loss of FA chains and abundant *m/z* 337.272 from the non-oxidized chain [MG 18:2+H-H_2O] and an oxidized moiety at 663.499 [M<O>+H-FA 18:2].

Overall, the current software for lipid annotation using rule-based fragmentation have a good performance, but the expansion of these rules for additional classes, especially for oxidized species, and the addition of a filter based on RT mapping can improve the number of true identifications and reduce the need for extensive manual curation. Furthermore, more

independent ring-trials are needed for lipid annotation tools, as most of them are based on comparisons conducted by their developers, which can be biased. The development of strategies for the automated annotation of oxidized lipids is advancing and probably manual curation will be less necessary in the future which could broaden the study on oxidized lipids involved in different biological conditions.

4. Concluding Remarks

For model organism studies, where several measurements are necessary using a limited amount of sample, the optimization of the analytical workflow is essential to obtain reliable results. Using zebrafish liver homogenates, a total of 712 unique lipids species from four categories (i.e., fatty acyls, glycerolipids, glycerophospholipids, and sphingolipids) were annotated with accurate mass, *in silico* MS/MS and RT mapping. Of those, 583, 565, and 575 lipid species were annotated in the extracts from the HE (MeOH/$CHCl_3$/H_2O, 3/2/2, v/v/v), MHE (MeOH/CH_2Cl_2/H_2O, 2/3/2, v/v/v) and ME (MeOH/MTBE/H_2O, 3/10/2.5, v/v/v) extraction methods, respectively. Both MHE and ME showed similar lipid coverage to HE and are suitable alternatives to chloroform-based extraction for zebrafish liver. Data-dependent acquisition using iterative exclusion MS/MS and active exclusion were used to increase the lipidome coverage by selecting a higher number of different precursor ions that are selected for MS/MS in each MS cycle. Lipostar was the identification software that showed the highest number of annotated lipids. Using open-source software, the combination of MS-DIAL and LipidMatch annotation using the same feature table combined with LipidHunter for confirmation could be used to annotate 515 different lipids from fourteen lipid subclasses. The lipids found in this work can be used in a larger context to help the lipidomics community gain a better understanding of model organism lipidomes.

Acknowledgments

Katyeny Manuela da Silva acknowledges a doctoral fellowship BOF DOCPRO 4 (Antigoon ID number 36893) from the University of Antwerp. Elias Iturrospe is funded by the Research Scientific Foundation-Flanders (FWO) – project number 1161620N. Rik van den Boom, Maria van de Lavoir and Rani Robeyns are funded by the University of Antwerp (BOF-GOA – PS ID 36572, BOF – Antigoon ID 46315 and BOF-GOA – PS ID 41667, respectively). The authors thank Julie Cools for her help during the homogenization of the samples.

Conflict of interest statement

The authors declare that they have no conflict of interest.

Data availability statement

Data files used for annotation converted to mzML format are available through the GNPS MassIVE repository (https://massive.ucsd.edu/ProteoSAFe/) with the data set identifier MSV000088860.

Supplementary Information

Supplementary information 1. Additional figures and tables used in this study.

Supplementary information 2. Lipid species annotated in zebrafish liver tissues using four software tools (Lipostar, MS-DIAL, LipidHunter, and LipidMatch) and three extraction methods (HE (MeOH/$CHCl_3$/H_2O, 3/2/2, v/v/v), MHE (MeOH/CH_2Cl_2/H_2O, 2/3/2, v/v/v) and ME (MeOH/MTBE/H_2O, 3/10/2.5, v/v/v).

References

Aldana, J., Romero-Otero, A., & Cala, M. P. (2020). Exploring the Lipidome: Current Lipid Extraction Techniques for Mass Spectrometry Analysis. *Metabolites*, *10*(6), 231. https://doi.org/10.3390/metabo10060231

Alseekh, S., Aharoni, A., Brotman, Y., Contrepois, K., D'Auria, J., Ewald, J., C. Ewald, J., Fraser, P. D., Giavalisco, P., Hall, R. D., Heinemann, M., Link, H., Luo, J., Neumann, S., Nielsen, J., Perez de Souza, L., Saito, K., Sauer, U., Schroeder, F. C., … Fernie, A. R. (2021). Mass spectrometry-based metabolomics: a guide for annotation, quantification and best reporting practices. *Nature Methods*, *18*(7), 747–756. https://doi.org/10.1038/s41592-021-01197-1

Arribat, Y., Grepper, D., Lagarrigue, S., Qi, T., Cohen, S., & Amati, F. (2020). Spastin mutations impair coordination between lipid droplet dispersion and reticulum. *PLOS Genetics*, *16*(4), e1008665. https://doi.org/10.1371/journal.pgen.1008665

Benchoula, K., Khatib, A., Jaffar, A., Ahmed, Q. U., Sulaiman, W. M. A. W., Wahab, R. A., & El-Seedi, H. R. (2019). The promise of zebrafish as a model of metabolic syndrome. *Experimental Animals*, *68*(4), 407–416. https://doi.org/10.1538/expanim.18-0168

Bligh, E. G., & Dyer, W. J. (1959). A Rapid Method of Total Lipid Extraction and Purification. *Canadian Journal of Biochemistry and Physiology*, *37*(8), 911–917. https://doi.org/10.1139/o59-099

519 Broadhurst, D., Goodacre, R., Reinke, S. N., Kuligowski, J., Wilson, I. D., Lewis, M. R., &
520 Dunn, W. B. (2018). Guidelines and considerations for the use of system suitability and
521 quality control samples in mass spectrometry assays applied in untargeted clinical
522 metabolomic studies. *Metabolomics*, *14*(6), 72. https://doi.org/10.1007/s11306-018-
523 1367-3
524 Cajka, T., & Fiehn, O. (2014). Comprehensive analysis of lipids in biological systems by
525 liquid chromatography-mass spectrometry. *TrAC - Trends in Analytical Chemistry*, *61*,
526 192–206. https://doi.org/10.1016/j.trac.2014.04.017
527 Criscuolo, A., Zeller, M., & Fedorova, M. (2020). Evaluation of Lipid In-Source
528 Fragmentation on Different Orbitrap-based Mass Spectrometers. *Journal of the*
529 *American Society for Mass Spectrometry*, *31*(2), 463–466.
530 https://doi.org/10.1021/jasms.9b00061
531 Cuykx, M., Mortelé, O., Rodrigues, R. M., Vanhaecke, T., & Covaci, A. (2017).
532 Optimisation of in vitro sample preparation for LC-MS metabolomics applications on
533 HepaRG cell cultures. *Analytical Methods*, *9*(24), 3704–3712.
534 https://doi.org/10.1039/c7ay00573c
535 Cuykx, M., Negreira, N., Beirnaert, C., Van den Eede, N., Rodrigues, R., Vanhaecke, T.,
536 Laukens, K., & Covaci, A. (2017). Tailored liquid chromatography–mass spectrometry
537 analysis improves the coverage of the intracellular metabolome of HepaRG cells.
538 *Journal of Chromatography A*, *1487*, 168–178.
539 https://doi.org/10.1016/j.chroma.2017.01.050
540 da Silva, K. M., Iturrospe, E., Bars, C., Knapen, D., Van Cruchten, S., Covaci, A., & van
541 Nuijs, A. L. N. (2021). Mass Spectrometry-Based Zebrafish Toxicometabolomics: A
542 Review of Analytical and Data Quality Challenges. *Metabolites*, *11*(9), 635.
543 https://doi.org/10.3390/metabo11090635
544 da Silva, K. M., Iturrospe, E., Heyrman, J., Koelmel, J. P., Cuykx, M., Vanhaecke, T.,
545 Covaci, A., & van Nuijs, A. L. N. (2021). Optimization of a liquid chromatography-ion
546 mobility-high resolution mass spectrometry platform for untargeted lipidomics and
547 application to HepaRG cell extracts. *Talanta*, *235*, 122808.
548 https://doi.org/10.1016/j.talanta.2021.122808
549 DeFelice, B. C., Mehta, S. S., Samra, S., Čajka, T., Wancewicz, B., Fahrmann, J. F., & Fiehn,
550 O. (2017). Mass Spectral Feature List Optimizer (MS-FLO): A Tool To Minimize False
551 Positive Peak Reports in Untargeted Liquid Chromatography–Mass Spectroscopy (LC-
552 MS) Data Processing. *Analytical Chemistry*, *89*(6), 3250–3255.

https://doi.org/10.1021/acs.analchem.6b04372

Ding, J., Ji, J., Rabow, Z., Shen, T., Folz, J., Brydges, C. R., Fan, S., Lu, X., Mehta, S., Showalter, M. R., Zhang, Y., Araiza, R., Bower, L. R., Lloyd, K. C. K., & Fiehn, O. (2021). A metabolome atlas of the aging mouse brain. *Nature Communications*, *12*(1), 6021. https://doi.org/10.1038/s41467-021-26310-y

Directive 2010/63/EU on the Protection of Animals Used for Scientific Purposes. (2010). *Official Journal of the European Union*. https://eur-lex.europa.eu/legal-content/EN/ALL/?uri=CELEX:32010L0063

Gegner, H. M., Mechtel, N., Heidenreich, E., Wirth, A., Cortizo, F. G., Bennewitz, K., Fleming, T., Andresen, C., Freichel, M., Teleman, A. A., Kroll, J., Hell, R., & Poschet, G. (2022). Deep Metabolic Profiling Assessment of Tissue Extraction Protocols for Three Model Organisms. *Frontiers in Chemistry*, *10*(April), 2021.12.16.472947. https://doi.org/10.3389/fchem.2022.869732

Goracci, L., Tortorella, S., Tiberi, P., Pellegrino, R. M., Di Veroli, A., Valeri, A., & Cruciani, G. (2017). Lipostar, a Comprehensive Platform-Neutral Cheminformatics Tool for Lipidomics. *Analytical Chemistry*, *89*(11), 6257–6264. https://doi.org/10.1021/ACS.ANALCHEM.7B01259/SUPPL_FILE/AC7B01259_SI_001.PDF

Hartler, J., Triebl, A., Ziegl, A., Trötzmüller, M., Rechberger, G. N., Zeleznik, O. A., Zierler, K. A., Torta, F., Cazenave-Gassiot, A., Wenk, M. R., Fauland, A., Wheelock, C. E., Armando, A. M., Quehenberger, O., Zhang, Q., Wakelam, M. J. O., Haemmerle, G., Spener, F., Köfeler, H. C., & Thallinger, G. G. (2017). Deciphering lipid structures based on platform-independent decision rules. *Nature Methods*, *14*(12), 1171–1174. https://doi.org/10.1038/nmeth.4470

Höring, M., Krautbauer, S., Hiltl, L., Babl, V., Sigruener, A., Burkhardt, R., & Liebisch, G. (2021). Accurate Lipid Quantification of Tissue Homogenates Requires Suitable Sample Concentration, Solvent Composition, and Homogenization Procedure—A Case Study in Murine Liver. *Metabolites*, *11*(6), 365. https://doi.org/10.3390/metabo11060365

Hyötyläinen, T. (2021). Analytical challenges in human exposome analysis with focus on environmental analysis combined with metabolomics. *Journal of Separation Science*, *44*(8), 1769–1787. https://doi.org/10.1002/jssc.202001263

Iturrospe, E., Da Silva, K. M., Robeyns, R., van de Lavoir, M., Boeckmans, J., Vanhaecke, T., van Nuijs, A. L. N., & Covaci, A. (2022). Metabolic Signature of Ethanol-Induced Hepatotoxicity in HepaRG Cells by Liquid Chromatography–Mass Spectrometry-Based

Untargeted Metabolomics. *Journal of Proteome Research*, *21*(4), 1153–1166. https://doi.org/10.1021/acs.jproteome.2c00029

Iturrospe, E., Da Silva, K. M., Talavera Andújar, B., Cuykx, M., Boeckmans, J., Vanhaecke, T., Covaci, A., & van Nuijs, A. L. N. (2021). An exploratory approach for an oriented development of an untargeted hydrophilic interaction liquid chromatography-mass spectrometry platform for polar metabolites in biological matrices. *Journal of Chromatography A*, *1637*, 461807. https://doi.org/10.1016/j.chroma.2020.461807

Klåvus, A., Kokla, M., Noerman, S., Koistinen, V. M., Tuomainen, M., Zarei, I., Meuronen, T., Häkkinen, M. R., Rummukainen, S., Farizah Babu, A., Sallinen, T., Kärkkäinen, O., Paananen, J., Broadhurst, D., Brunius, C., & Hanhineva, K. (2020). "Notame": Workflow for Non-Targeted LC–MS Metabolic Profiling. *Metabolites*, *10*(4), 135. https://doi.org/10.3390/metabo10040135

Koelmel, J. P., Kroeger, N. M., Gill, E. L., Ulmer, C. Z., Bowden, J. A., Patterson, R. E., Yost, R. A., & Garrett, T. J. (2017). Expanding Lipidome Coverage Using LC-MS/MS Data-Dependent Acquisition with Automated Exclusion List Generation. *Journal of the American Society for Mass Spectrometry*, *28*(5), 908–917. https://doi.org/10.1007/s13361-017-1608-0

Koelmel, J. P., Kroeger, N. M., Ulmer, C. Z., Bowden, J. A., Patterson, R. E., Cochran, J. A., Beecher, C. W. W., Garrett, T. J., & Yost, R. A. (2017). LipidMatch: An automated workflow for rule-based lipid identification using untargeted high-resolution tandem mass spectrometry data. *BMC Bioinformatics*, *18*(1), 331. https://doi.org/10.1186/s12859-017-1744-3

Köfeler, H. C., Eichmann, T. O., Ahrends, R., Bowden, J. A., Danne-Rasche, N., Dennis, E. A., Fedorova, M., Griffiths, W. J., Han, X., Hartler, J., Holčapek, M., Jirásko, R., Koelmel, J. P., Ejsing, C. S., Liebisch, G., Ni, Z., O'Donnell, V. B., Quehenberger, O., Schwudke, D., … Ekroos, K. (2021). Quality control requirements for the correct annotation of lipidomics data. *Nature Communications*, *12*(1), 4771. https://doi.org/10.1038/s41467-021-24984-y

Korf, A., Jeck, V., Schmid, R., Helmer, P. O., & Hayen, H. (2019). Lipid Species Annotation at Double Bond Position Level with Custom Databases by Extension of the MZmine 2 Open-Source Software Package. *Analytical Chemistry*, *91*(8), 5098–5105. https://doi.org/10.1021/ACS.ANALCHEM.8B05493/SUPPL_FILE/AC8B05493_SI_003.PDF

Kotronen, A., Seppänen-Laakso, T., Westerbacka, J., Kiviluoto, T., Arola, J., Ruskeepää, A.-

L., Yki-Järvinen, H., & Orešič, M. (2010). Comparison of Lipid and Fatty Acid Composition of the Liver, Subcutaneous and Intra-abdominal Adipose Tissue, and Serum. *Obesity*, *18*(5), 937–944. https://doi.org/10.1038/oby.2009.326

Lai, K. P., Gong, Z., & Tse, W. K. F. (2021). Zebrafish as the toxicant screening model: Transgenic and omics approaches. *Aquatic Toxicology*, *234*, 105813. https://doi.org/10.1016/j.aquatox.2021.105813

Lange, M., Angelidou, G., Ni, Z., Criscuolo, A., Schiller, J., Blüher, M., & Fedorova, M. (2021). AdipoAtlas: A reference lipidome for human white adipose tissue. *Cell Reports Medicine*, *2*(10), 100407. https://doi.org/10.1016/j.xcrm.2021.100407

Lange, M., Ni, Z., Criscuolo, A., & Fedorova, M. (2019). Liquid Chromatography Techniques in Lipidomics Research. *Chromatographia*, *82*(1), 77–100. https://doi.org/10.1007/s10337-018-3656-4

Lebold, K. M., Kirkwood, J. S., Taylor, A. W., Choi, J., Barton, C. L., Miller, G. W., Du, J. La, Jump, D. B., Stevens, J. F., Tanguay, R. L., & Traber, M. G. (2014). Novel liquid chromatography-mass spectrometry method shows that vitamin E deficiency depletes arachidonic and docosahexaenoic acids in zebrafish (danio rerio) embryos. *Redox Biology*, *2*(1), 105–113. https://doi.org/10.1016/j.redox.2013.12.007

Liebisch, G., Fahy, E., Aoki, J., Dennis, E. A., Durand, T., Ejsing, C. S., Fedorova, M., Feussner, I., Griffiths, W. J., Köfeler, H., Merrill, A. H., Murphy, R. C., O'Donnell, V. B., Oskolkova, O., Subramaniam, S., Wakelam, M. J. O., Spener, F., O, V. B., Oskolkova, O., … Spener, F. (2020). Update on LIPID MAPS classification, nomenclature, and shorthand notation for MS-derived lipid structures. *Journal of Lipid Research*, *61*(12), 1539–1555. https://doi.org/10.1194/jlr.S120001025

Liebisch, G., Vizcaíno, J. A., Köfeler, H., Trötzmüller, M., Griffiths, W. J., Schmitz, G., Spener, F., & Wakelam, M. J. O. (2013). Shorthand notation for lipid structures derived from mass spectrometry. *Journal of Lipid Research*, *54*(6), 1523–1530. https://doi.org/10.1194/jlr.M033506

Liu, Z., Wang, P., Liu, Z., Wei, C., Li, Y., & Liu, L. (2021). Evaluation of liver tissue extraction protocol for untargeted metabolomics analysis by ultra-high-performance liquid chromatography/tandem mass spectrometry. *Journal of Separation Science*, *44*(18), 3450–3461. https://doi.org/10.1002/jssc.202100051

Matyash, V., Liebisch, G., Kurzchalia, T. V, Shevchenko, A., & Schwudke, D. (2008). Lipid extraction by methyl-tert-butyl ether for high-throughput lipidomics. *Journal of Lipid Research*, *49*(5), 1137–1146. https://doi.org/10.1194/jlr.D700041-JLR200

Michiels, E. D. G., Vergauwen, L., Lai, F. Y., Town, R. M., Covaci, A., van Nuijs, A. L. N., Van Cruchten, S. J., & Knapen, D. (2019). Advancing the Zebrafish embryo test for endocrine disruptor screening using micro-injection: Ethinyl estradiol as a case study. *Environmental Toxicology and Chemistry*, *38*(3), 533–547. https://doi.org/10.1002/etc.4343

Murphy, R. C. (2014). Tandem Mass Spectrometry of Lipids. In *New Developments in Mass Spectrometry*. Royal Society of Chemistry. https://doi.org/10.1039/9781782626350

Narváez-Rivas, M., & Zhang, Q. (2016). Comprehensive untargeted lipidomic analysis using core–shell C30 particle column and high field orbitrap mass spectrometer. *Journal of Chromatography A*, *1440*, 123–134. https://doi.org/10.1016/J.CHROMA.2016.02.054

Ni, Z., Angelidou, G., Hoffmann, R., & Fedorova, M. (2017). LPPtiger software for lipidome-specific prediction and identification of oxidized phospholipids from LC-MS datasets. *Scientific Reports*, *7*(1), 15138. https://doi.org/10.1038/s41598-017-15363-z

Ni, Z., Angelidou, G., Lange, M., Hoffmann, R., & Fedorova, M. (2017). LipidHunter Identifies Phospholipids by High-Throughput Processing of LC-MS and Shotgun Lipidomics Datasets. *Analytical Chemistry*, *89*(17), 8800–8807. https://doi.org/10.1021/acs.analchem.7b01126

Reinicke, M., Dorow, J., Bischof, K., Leyh, J., Bechmann, I., & Ceglarek, U. (2020). Tissue pretreatment for LC–MS/MS analysis of PUFA and eicosanoid distribution in mouse brain and liver. *Analytical and Bioanalytical Chemistry*, *412*(10), 2211–2223. https://doi.org/10.1007/S00216-019-02170-W/FIGURES/5

Sands, C. J., Gómez-Romero, M., Correia, G., Chekmeneva, E., Camuzeaux, S., Izzi-Engbeaya, C., Dhillo, W. S., Takats, Z., & Lewis, M. R. (2021). Representing the Metabolome with High Fidelity: Range and Response as Quality Control Factors in LC-MS-Based Global Profiling. *Analytical Chemistry*, *93*(4), 1924–1933. https://doi.org/10.1021/acs.analchem.0c03848

Sun, L., Ling, Y., Jiang, J., Wang, D., Wang, J., Li, J., Wang, X., & Wang, H. (2020). Differential mechanisms regarding triclosan vs. bisphenol A and fluorene-9-bisphenol induced zebrafish lipid-metabolism disorders by RNA-Seq. *Chemosphere*, *251*, 126318. https://doi.org/10.1016/J.CHEMOSPHERE.2020.126318

Tsugawa, H., Ikeda, K., Takahashi, M., Satoh, A., Mori, Y., Uchino, H., Okahashi, N., Yamada, Y., Tada, I., Bonini, P., Higashi, Y., Okazaki, Y., Zhou, Z., Zhu, Z.-J. J., Koelmel, J., Cajka, T., Fiehn, O., Saito, K., Arita, M. M., & Arita, M. M. (2020). A lipidome atlas in MS-DIAL 4. *Nature Biotechnology*, *38*(10), 1159–1163.

https://doi.org/10.1038/s41587-020-0531-2

Ulmer, C. Z., Jones, C. M., Yost, R. A., Garrett, T. J., & Bowden, J. A. (2018). Optimization of Folch, Bligh-Dyer, and Matyash sample-to-extraction solvent ratios for human plasma-based lipidomics studies. *Analytica Chimica Acta*, *1037*, 351–357. https://doi.org/10.1016/j.aca.2018.08.004

Wickham, H. (2016). *ggplot2: Elegant Graphics for Data Analysis*. Springer-Verlag New York. https://ggplot2.tidyverse.org

Witting, M., & Böcker, S. (2020). Current status of retention time prediction in metabolite identification. *Journal of Separation Science*, *43*(9–10), 1746–1754. https://doi.org/10.1002/JSSC.202000060

Wu, Z. E., Kruger, M. C., Cooper, G. J. S., Poppitt, S. D., & Fraser, K. (2019). Tissue-Specific Sample Dilution: An Important Parameter to Optimise Prior to Untargeted LC-MS Metabolomics. *Metabolites*, *9*(7), 124. https://doi.org/10.3390/metabo9070124

Figures

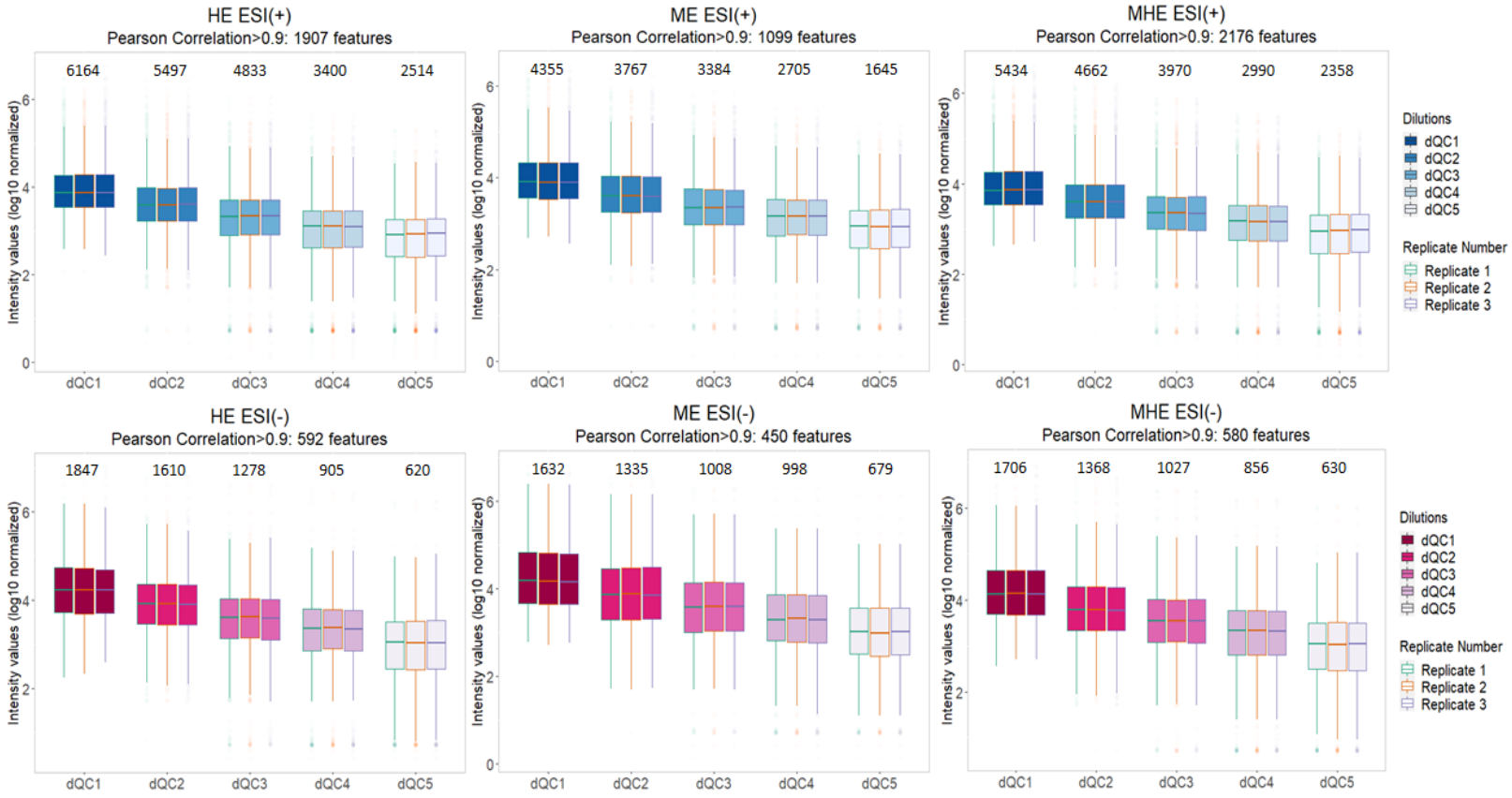

Figure 1. Dilution series (dilution factor = 2) of zebrafish liver extracts with different extraction solvents analyzed by LC-HRMS. The replicate number refers to instrumental injections. The numbers at the top of each bar refer to the number of features with a relative standard deviation of the intensity ≤ 10%. HE: In house extraction, MeOH/$CHCl_3$/H_2O (3/2/2, v/v/v). MHE: Modified in house extraction, MeOH/CH_2Cl_2/H_2O (2/3/2, v/v/v). ME: Matyash extraction, MeOH/MTBE/H_2O (3/10/2.5, v/v/v).

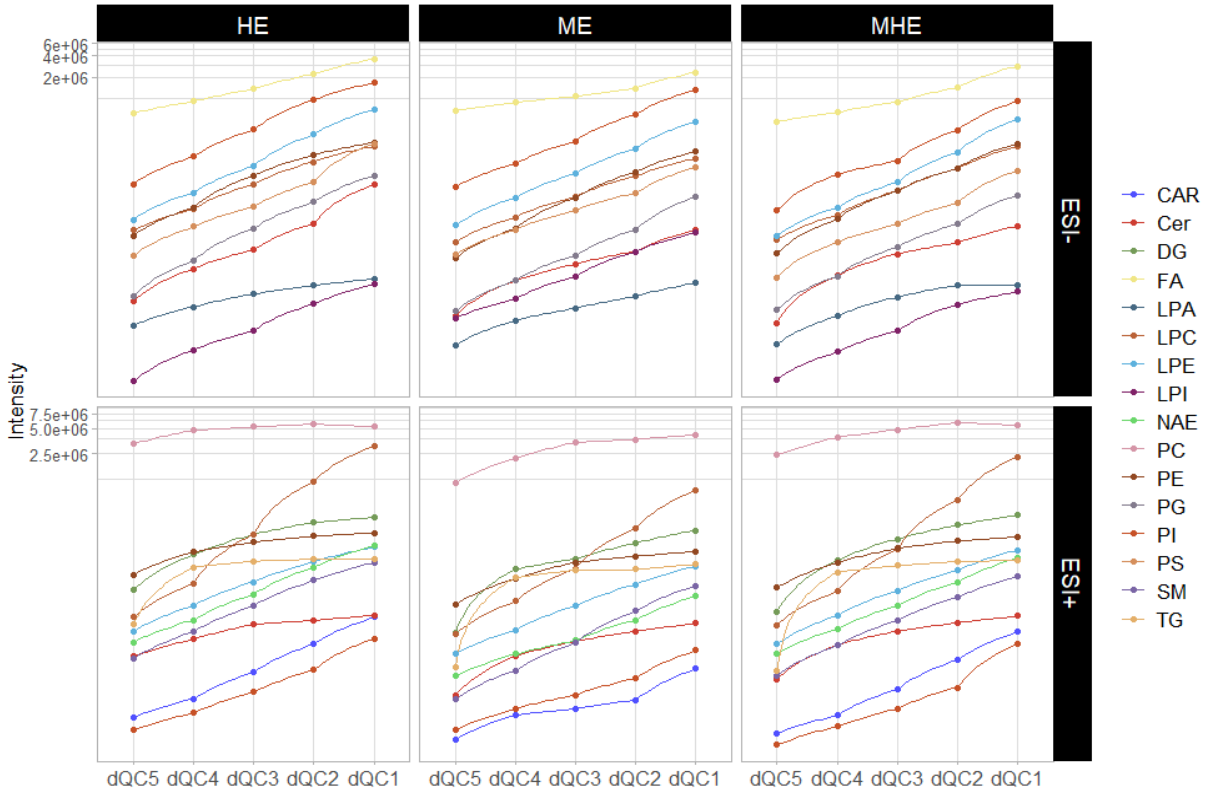

Figure 2. The intensity of annotated lipid categories from different lipid classes in zebrafish liver homogenates. The shown mean intensities were calculated based on the most abundant ionization species for each lipid species within a lipid category. The y axis was log-transformed. HE: In house extraction, MeOH/$CHCl_3$/H_2O (3/2/2, v/v/v). MHE: Modified in house extraction, MeOH/CH_2Cl_2/H_2O (2/3/2, v/v/v). ME: Matyash extraction, MeOH/MTBE/H_2O (3/10/2.5, v/v/v).

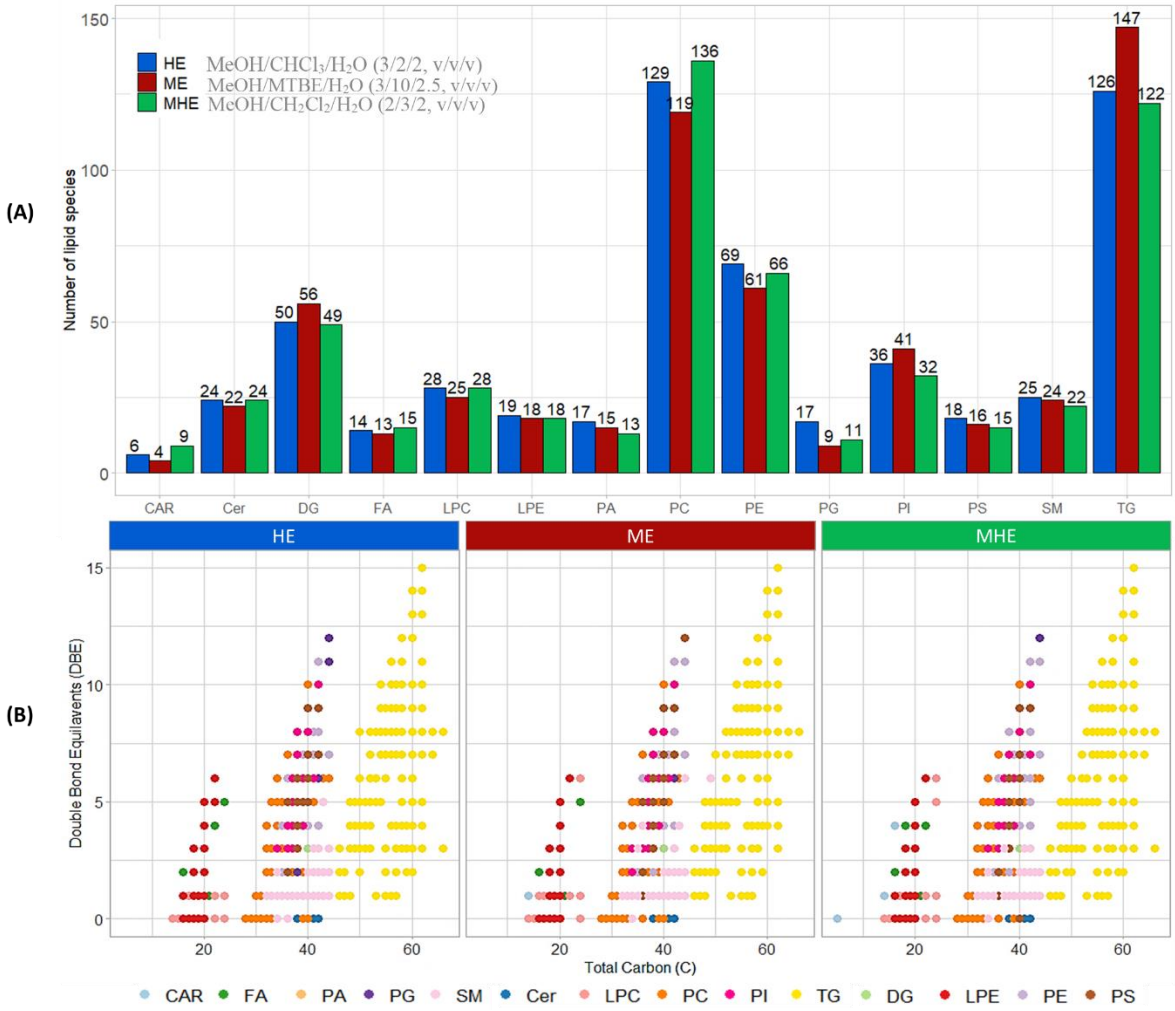

719

720 **Figure 3**. Annotated lipids in zebrafish liver homogenates with different extractions (HE,
721 MHE, and ME) **(A)** and their double bond equivalents (DBE) plotted against the number of
722 carbons (total carbon (C)) **(B)**.

723

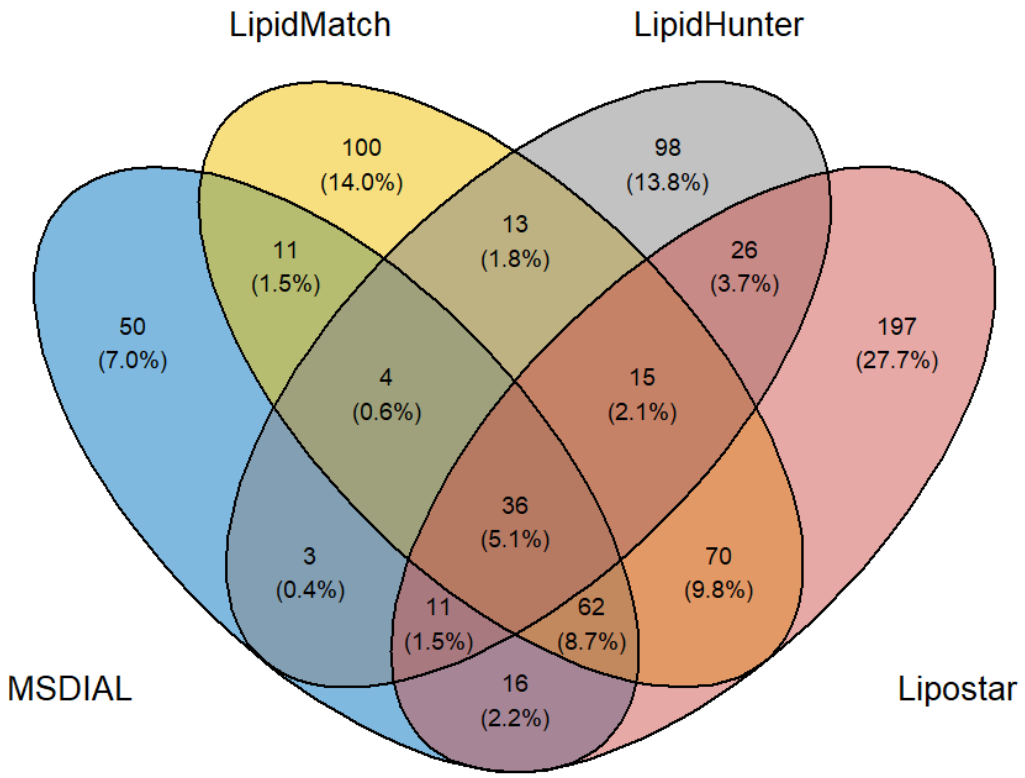

724

725 **Figure 4.** Venn diagram of the number of annotated lipid species using different software tools.

726